Journal of Polytechnic, 2017; 20 (2) : 487-494

Modeling and Analysis of a Microfluidic Capillary Valve

Ender YILDIRIM*

Çankaya University, Mechanical Engineering Department

(Received : 07.07.2016 ; Accepted : 24.10.2016)

ABSTRACT

Here, a numerical model for analysis of a capillary valve for use in microfluidic devices was presented. Capillary valves are preferred especially in passive microfluidic systems, where the capillary forces dominate the liquid motion, to manipulate the flow. The capillary valve in this work, was formed by the sudden expansion of a rectangular microchannel to an opening, whose depth and width are larger than the height and the width of the channel respectively. Noting that there was no available analytical model to determine the pressure capacity of such valves, a numerical model based on energy minimization was utilized. Free software Surface Evolver was used to solve the model. Dependence of the pressure capacity on the contact angle of the working liquid on the channel material was investigated. It was found that the pressure capacity of the valves would be maximum if the contact angle on all surfaces is 90º. Accordingly, the valves could withstand approximately 2.5 kPa for 100 μm × 100 μm channels when the contact angle was 90º. The model was verified by comparing the results with those available in the literature.

Keywords: Microfluidic, Capillary Valve, Pressure Capacity, Contact Angle.

ÖZ

Burada, mikroakışkan cihazlarda kullanılan kılcal valflerin analizi için bir numerik model sunulmuştur. Kılcal valfler, özellikle kılcal kuvvetlerin baskın olduğu pasif mikroakışkan sistemlerde, akışı yönlendirmek için tercih edilirler. Bu çalışmadaki kılcal valf, dikdörtgen kesitli bir mikrokanalın, derinliği ve genişliği kanalın yüksekliği ve genişliğinden daha fazla olan bir açıklığa doğru aniden genişlemesi ile oluşmaktadır. Bu şekildeki valflerin basınç kapasitesini belirlemek için herhangi bir analitik modelin bulunmaması göz önünde bulundurularak, enerji enazlamaya dayalı bir numerik model kullanılmıştır. Modelin çözümü için ücretsiz bir yazılım olan Surface Evolver kullanılmıştır. Basınç kapasitesinin, çalışma sıvısının kanal malzemesi üzerindeki temas açısı ile ilişkisi incelenmiştir. Tüm yüzeylerde temas açısının 90º olması durumunda basınç kapasitesinin en yüksek olacağı belirlenmiştir. Buna bağlı olarak, 100 μm × 100 μm kesitli kanallar için temas açısı 90º olduğunda valfler yaklaşık 2.5kPa'ya çıkabilmektedir. Model, sonuçların literatürdeki sonuçlarla karşılaştırılması ile doğrulanmıştır.

Anahtar Kelimeler: Mikroakışkan, Kılcal Valf, Basınç Kapasitesi, Temas Açısı.

1. INTRODUCTION

Microfluidics relates to handling minute amounts of liquids (microliters to nanoliters) within channels of characteristics dimensions in the order of 10^1-10^2 μm. Due to the fabrication methods, the channels in microfluidic devices often have rectangular cross section. Microfluidics is commonly perceived as an enabling technology especially for chemical and biological applications. In these applications, it is often required to manipulate the flow of different reagents and/or samples on the microfluidic device, commonly called as the lab-on-a-chip. For this purpose, researchers have developed various active or passive microvalves [1]. Among these, especially the capillary valves are of interest since they are typically passive and hence easy to operate, and they often do not involve any moving part, thus they are easy to implement.

Capillary valves function as pressure barriers, where an advancing meniscus stops due to an acute change in the hydrophilicity of the surface or in the channel geometry. In ref. [2, 3] hydrophobic coatings were patterned at the bottom of microchannels, where the liquid advancing was blocked due to decreased tension at the solid coating-liquid interface. On the other hand, in ref. [4–6], diverging channels were utilized as capillary valves. Here, sudden expansion of the channel at diverging section causes the liquid meniscus to be pinned at the beginning of the expansion. In these studies, the expansions were implemented by simply widening the microchannel while keeping the channel height constant. Sudden expansion by increasing the height of the channel was also reported in the literature [7]. An interesting and easy-to-implement example of capillary valves was presented in ref. [8], where the side wall of the microchannel were patterned to define an acute change in the cross section. Alternatively, in ref. [9] ridges were patterned at the bottom of the microchannel, which acted as pressure barriers.

In this paper, capillary valves utilizing an abrupt increase in the cross-sectional area were considered (Figure 1a-b). Basically, when a meniscus advancing in a microchannel faces an opening (*capillary valve*) with a cross sectional area greater than that of the channel, the sharp bend on the channel boundary causes a sudden increase in the apparent contact angle ($90^o + \theta_1$ as illustrated on Figure 1c, considering the meniscus shape at the onset of

*Corresponding Author
e-mail: endery@cankaya.edu.tr
Digital Object Identifier (DOI) : 10.2339/2017.20.2 487-494

overflow). For the meniscus to advance through the opening, pressure must develop within the liquid, which in turn stretches the meniscus. After a certain pressure (henceforth it will be called the *pressure capacity*), the meniscus overflows the capillary valve. This explanation of the capillary valve overflow is often called as capillary burst. However, since the breaching of the capillary valve is a transient process involving the stretching of the meniscus rather than a sudden bursting, *overflow* term will be used instead of bursting in this paper. Figure 1c illustrates this overflow process.

Examining the literature yields that there is still no analytical model to accurately determine the pressure capacity of these particular capillary valves [10]. Besides, available numerical models describing the behavior of these capillary valves do not consider the overflow process. Thus, a model describing the meniscus geometry during overflow of the capillary valve and corresponding pressure capacity is highly needed. In this paper, a numerical method, which models the meniscus geometry during overflow was presented. The model also relates the geometry of the meniscus to the pressure capacity of the capillary valve.

Considering that these capillary valves could be fabricated by using different techniques and materials, the model was first utilized to investigate the effect of wetting properties of the channel material (hence the contact angle) on the pressure capacity of the valves. After determining the proper contact angle for the best performing valves (corresponding to the highest pressure capacity), effect of channel dimensions was examined by simulating a range of channels with varying depth and width. Finally, the results were compared to experimental and theoretical values reported previously in the literature to verify the method presented here.

2. MODEL

For the capillary valve of interest to be functional, Concus-Finn criterion [11, 12] (Equation 1), which relates the bend angle and the contact angle of the liquid on the channel material and on the cover material (β, θ_1, and θ_2 respectively on Figure 1c), must be met.

$$\beta \geq 180^{o} - \left(\theta_1 - \theta_2\right) \tag{1}$$

Concus-Finn criterion in Equation 1 was originally developed for describing behavior of meniscus in wedge. However, it was shown in ref. [12] that this relation can as well be used to describe meniscus stretching on pressure barriers similar to the one illustrated in Figure 1a owing to the wedge-like shape formed by the channel cover and the front wall on the opening (Figure 1a).

Although, 2D illustration in Figure 1c describes the basics of the operation, it does not provide an information about the pressure capacity of the capillary valve. The pressure developed at any capillary interface is given by Young-Laplace law (Equation 2), which states that the pressure across a capillary interface is proportional to mean curvature of the interface and the proportionality constant is the surface tension.

$$P = \sigma\left(\frac{1}{R_1} + \frac{1}{R_2}\right) \tag{2}$$

Here, P is the pressure across the capillary interface, σ is the surface tension, R_1 and R_2 are the principle radii describing the curvature of the meniscus. It should be noted that, principle radii of curvature can only be determined through examining the 3D shape of the meniscus. Therefore, a 3D analysis must be carried out to fully understand the overflow behavior of the capillary valves and their respective pressure capacities.

Various analytical approaches to estimate the pressure capacity in similar capillary valves, where diverging channels with uniform height, have been presented in the literature [4–6]. However, there is no analytical model available for the valves considered in this paper. Moreover, some of the existing models for the other capillary valves do not consider the *corner filling* effect during overflow, which was first described by Concus and Finn in ref. [11]. Depending on the contact angle of the liquid on the channel material and cover material (θ_1 and θ_2 respectively in Figure 1c), the liquid tends to advance along the corner formed by the front wall and the top wall (stated as corner filling in Figure 1d) [13, 14]. Depending on the contact angles θ_1 and θ_2, corner filling effect may result in very intricate meniscus shapes during overflow, which is illustrated in Figure 1d.

The author had previously developed an analytical model to describe the 3D shape of a meniscus overflowing a particular type of capillary valve; phaseguide [9], which is in the form of a shallow ridge located at the bottom of a microchannel. In case of phaseguide overflow, meniscus advancing is only in the direction of the channel axis. On the other hand, since meniscus advancing during overflow is not unidirectional in case of the capillary valves considered in this paper (as illustrated in Figure 1d), this model cannot be used here. Instead, a numerical approach was utilized in this paper to determine the meniscus shape during overflow of the capillary valve and respective pressure capacity.

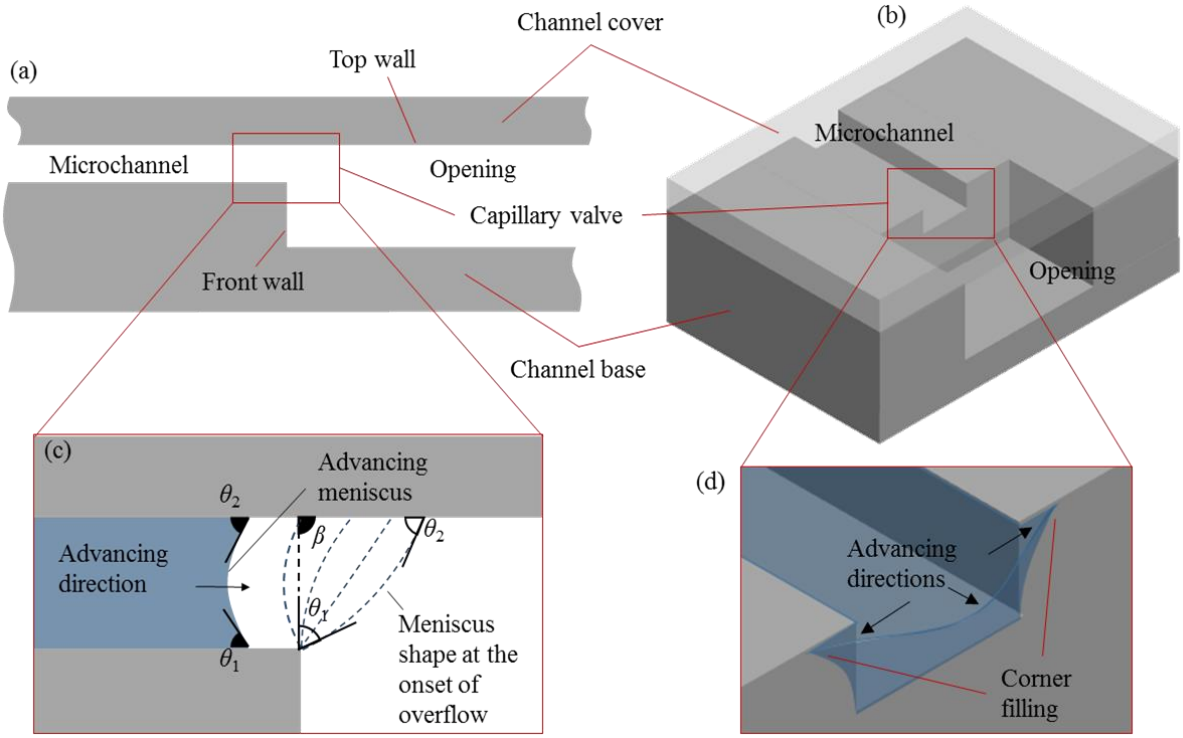

Figure 1. Capillary valve considered in this paper. (a) Profile view and (b) isometric view of the valve. Intersection of a rectangular microchannel and an opening, whose depth and width are larger than the height and the width of the channel respectively, forms the microchannel. A meniscus advancing in the microchannel gets pinned at the edges of this intersection. (c) Profile view illustrating the 2D understanding of the mensicus pinning and the overflow. (d) Isometric view of the meniscus pinned at the capillary valve, showing the corner filling effect and the meniscus advancing directions in 3D explanation of overflow.

Here, a freely available software – the Surface Evolver – was used to determine the meniscus shape. The Surface Evolver developed by K.A. Brakke, computes the shapes of the surfaces under surface tension, gravity, or other forms by minimizing the surface energy [15]. For this purpose, the Surface Evolver utilizes a finite-element approach, where the surface is divided into triangular facets. Surface energy (E) of a facet under surface tension, gravity, and a pressure difference across the facet can be stated as [15]:

$$E = \int_S \sigma \mathbf{k} \cdot d\mathbf{S} + g\rho \int_S \frac{z^2}{2} \mathbf{k} \cdot d\mathbf{S} - P \int_S z\mathbf{k} \cdot d\mathbf{S} \qquad (3)$$

where σ is the surface tension, g is the gravitational acceleration, ρ is the density of the liquid, P is the pressure across the facet, $\mathbf{k}$ is the surface normal vector defining the facet, z is the nodal position defining the facet, $d\mathbf{S}$ is the differential facet area, and S is the surface area of the interface. Here, it should be noted that although the gravity acts on the body instead of the surface, gravitational energy can be calculated through surface integral by utilizing divergence theorem [15]. On the other hand, considering that gravity often has a negligible effect due to the scale of the microfluidics, the second term on the right-hand side of Equation 3 was neglected in computation. Hence the surface energy becomes

$$E = \int_S \sigma \mathbf{k} \cdot d\mathbf{S} - P \int_S z\mathbf{k} \cdot d\mathbf{S} \qquad (4)$$

The Surface Evolver minimizes this energy given in Equation 4 by incrementally moving the vertices of the facets until the change in the surface energy is less than a specified error. Thus, the pressure across the meniscus (P) can be computed in relation to the meniscus shape.

For this purpose, an initial approximate geometry describing the shape of the meniscus pinned at the capillary valve was modeled (Figure 2a). Here it should be noted that the surface of the liquid in the microchannel was not included in the model since its boundaries were fixed (walls of the microchannel), thus it had no contribution in variation of the surface energy. Boundary conditions of the model and faceted boundaries are shown in Figure 2a.

To determine the pressure capacity of the capillary valve and the shape of the meniscus during overflow, initially the pressure across the meniscus (P in Equation 4) was set to zero. Then, the meniscus was evolved to minimize the surface energy until the relative change in the energy is less than 1×10^{-4}. Resulting shape was determined as the meniscus shape at zero pressure. After then, the pressure was sequentially increased at small increments and respective meniscus shapes were determined. This procedure was carried out until the meniscus totally

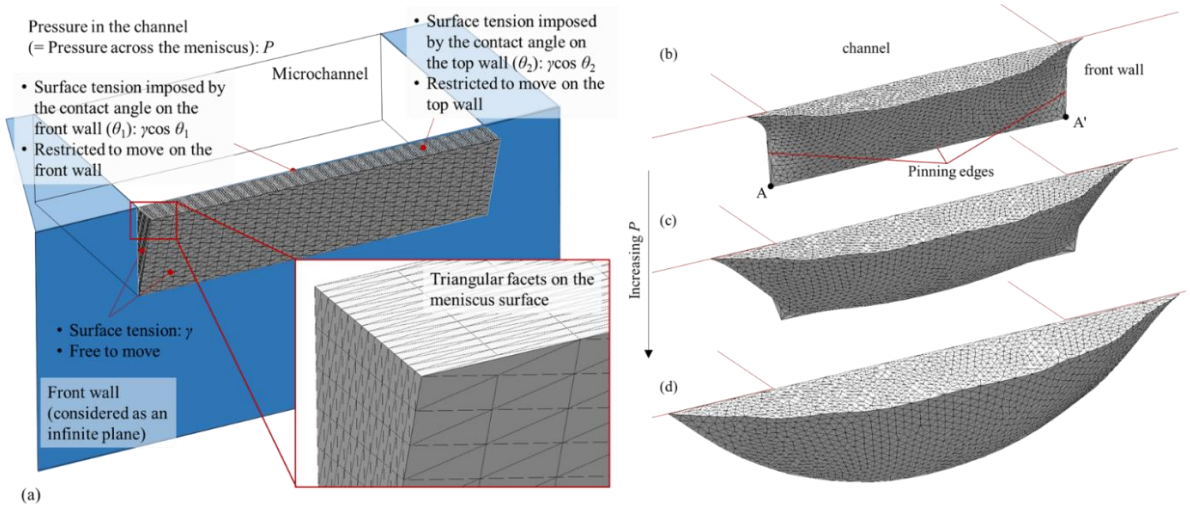

Figure 2. (a) Surface Evolver model of the meniscus and respective boundary conditions. The meniscus was modeled as a wedge leaning slightly out from the capillary valve. Surface of the meniscus was meshed by using triangular facets. Boundary conditions on the surfaces were explained on the figure. Top wall and the front wall were shaded in blue to improve visualization. (b)-(d) Meniscus shape during overflow of a specific valve (channel width: 400 µm, channel height: 100 µm, $\theta_1 = \theta_2 = 60^o$). As the pressure in the channel (P) increases, the mensicus first tends to advance along the corner formed by the top wall and the front wall, while being trapped at the pinning edges. Overflow occurs when the meniscus breaches points A and A'.

breaches the capillary valve. The pressure at this point was identified as the pressure capacity of the capillary valve. Figure 2b illustrates the procedure by showing the shape of the meniscus during overflow of a specific capillary valve.

3. RESULTS

Numerical method described in the previous section was carried out for combinations of top wall and channel wall contact angles (θ_1 and θ_2 respectively). The motivation behind doing so was based on the common microfluidic fabrication techniques. Although there are a number of methods for fabricating microfluidic devices [16], especially one of these methods – PDMS (polydimethylsiloxane) molding [17] – is common because of its robustness and fairly rapid processing. In this method, PDMS resin is poured on a mold, which defines the channel geometry, and then cured under elevated temperature. After then, PDMS channel is sealed with a glass substrate by plasma assisted bonding process. Despite the advantages offered by the process, undesired properties of the material such as vapor permeability and uncontrolled wettability in long term use, limits the use of PDMS molded microfluidic devices to rapid prototyping only. For fabrication of commercial microfluidic devices, channels are often patterned on thermoplastic substrates such as polymethylmethacrylate (PMMA) or cyclic olefin copolymer (COC) by injection molding or hot embossing [18]. Patterned channels are then sealed with a blank thermoplastic substrate by thermo-compressive bonding. Figure 3a illustrates these fabrication techniques. Noting that different materials (commonly glass or thermoplastics) can be used to seal the channels fabricated on different materials (commonly PDMS or thermoplastics), combination of top wall and channel wall contact angles were considered in the analysis of the capillary valves.

Contact angle of water on these substrates (glass, PDMS, and PMMA as a representative thermoplastic material) were measured to illustrate the parameter range (Figure 3b). Accordingly, contact angles on top wall and channel wall were selected as ranging between 30° and 90°. On the other hand, channel width and height were kept constant at 400 µm and 100 µm respectively, which are representative values for a typical microfluidic channel. Water was assumed as the working liquid in all the simulations. List of parameters is shown in Table 1.

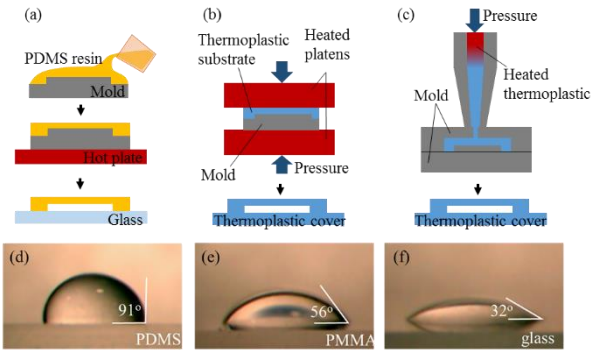

Figure 3. (a)-(c) Illustration of common microfluidic fabrication techniques: (a) PDMS molding, (b) hot embossing, and (c) injection molding. (d)-(f) Contact angle of water measured on (a) PDMS, (b) PMMA, and (c) glass.

Table 1. Parameters and variables tested in the simulations, and their corresponding values.

Parameter/variable name	Value
Contact angle on channel wall, θ_1	30°, 60°, 90°
Contact angle on top wall, θ_2	30°, 60°, 90°
Channel depth, d	100 µm
Channel width, w	400 µm
Surface tension of water, σ	0.073 J/m^2

The simulations were run on a workstation with 2.60 GHz dual processor and 16 GB RAM. Before running the simulations, mesh dependency was checked to ensure the convergence and accuracy of the results. Accordingly, it was decided to run the simulations on the models with approximately 3500 triangular facets. Figure 4a shows the simulated shapes of menisci at the onset of overflow for different contact angles and Figure 4b plots the corresponding pressure capacities.

Investigating the results reveals that the pressure capacity increases with increasing contact angle (both on top wall and channel wall) as implied by the Concus-Finn condition in equation 1. On the other hand, Figure 4b shows that the effect of the contact angle on the top wall dominates the effect of that on the channel wall. Indeed, this results is obvious since the meniscus pinned at the capillary valve can advance freely on the top wall only. Another conclusion that can be drawn from the simulation results is related to the corner filling effect. It can be seen from Figure 4a that especially for relatively low contact angle combinations, the meniscus tends to advance along the corner formed by the top and the front walls before the meniscus breaches the capillary valve. Thus, although Concus-Finn condition in Equation 1 states that the sum of the contact angles on top wall and the channel wall should be greater than 90° for this particular valve to be operational, non-zero pressure capacity can be obtained even when this condition is not satisfied. However, since the pressure capacities for these specific cases ($\theta_1 + \theta_2 \leq 90^o$) are very low, it will probably not be feasible to utilize these specific valves.

The results show that the highest pressure capacity can be obtained when the contact angle on all surfaces is 90°, which is possible if the capillary valve is fabricated by PDMS molding (Figure 3a) and sealed by another PDMS slab. Therefore, to investigate the effect of the channel dimensions on the valve performance, a number of simulations were carried out by changing the channel

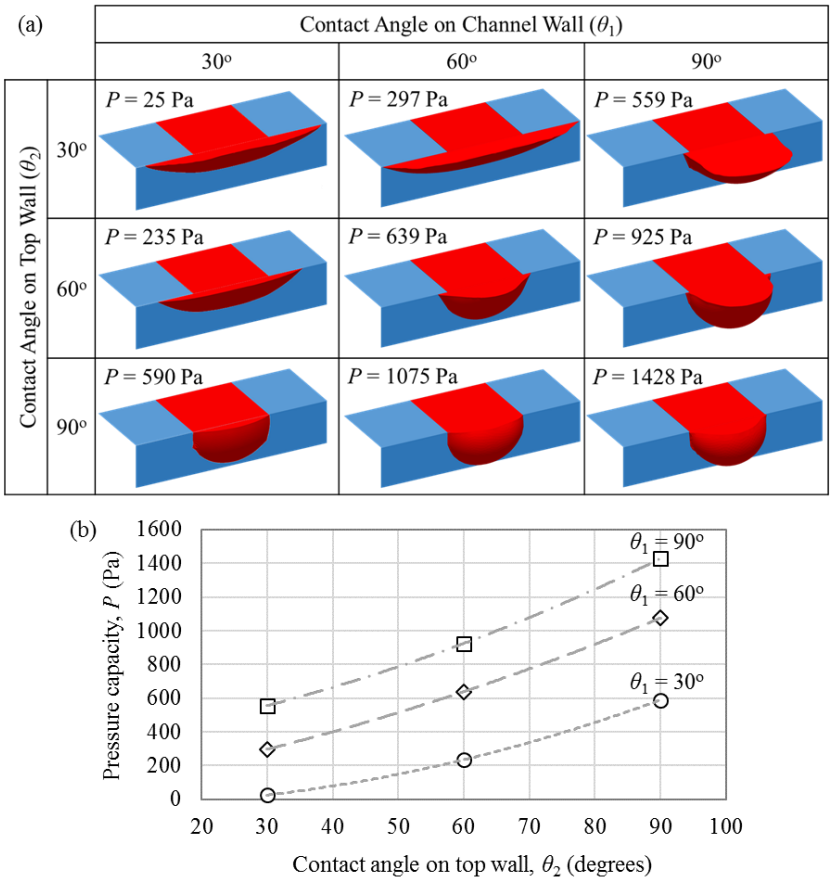

Figure 4. (a) Meniscus shapes computed by the Surface Evolver at the onset of overflow for different contact angle combinations. (b) Corresponding pressure capacities. Dashed lines on the plot indicates the trendlines fitted to the experimental data.

width and depth between 100 µm and 500 µm while keeping the contact angle constant at 90º. Figure 5 shows the change of the pressure capacity with respect to channel width and depth. Examining the results shows that decreasing the width and height improves the pressure capacity. It can be stated that either decreasing the width or the depth does not make a significant change in the increase of the pressure capacity. However, a careful investigation shows that increasing the channel width is slightly more effective than increasing the depth. This result is quite reasonable, since increasing the width does not only increase the surface on which the liquid can advance on the front wall (Figure 2a), but also the top surface, where the meniscus can stretch.

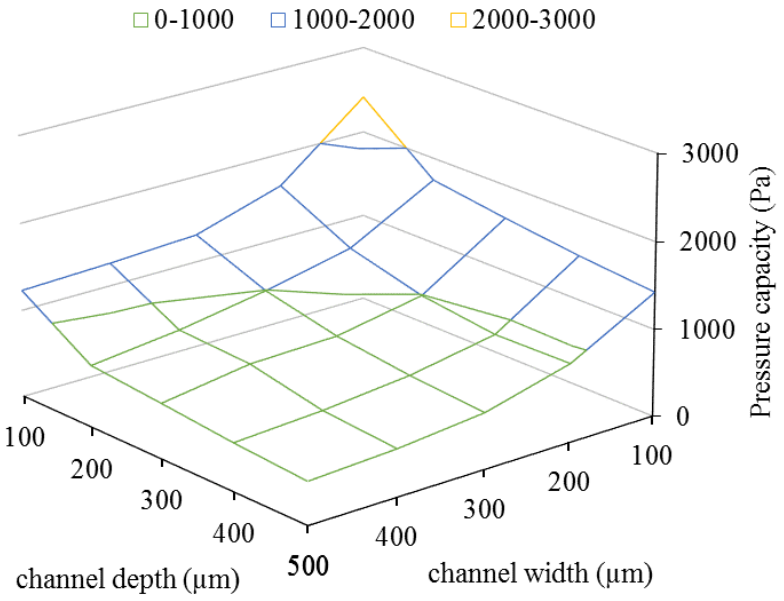

Figure 5. Pressure capacity of the capillary valve with respect to the channel depth and the channel width. Contact angle on all surfaces is

To verify the analysis method presented above, the results were compared to those presented in ref. [10], where another numerical approach, which utilized free surface equilibrium analysis [19] instead of energy minimization, was presented. For this purpose, θ_1 and θ_2 were kept constant at 60º and 80º respectively and the channel height was set to 15 µm, while varying the channel width between 30 µm and 115 µm. The results were plotted in Figure 6. It can be seen that the pressure capacities computed by using the method presented here are slightly larger than those presented in ref. [10]. This difference was attributed to one main reason, which is related to the definition of the overflow. In ref. [10], the authors define bursting as the state, when the contact angle measured at the mid-point of the pinning edge formed by the intersection of the channel bottom and the front wall, becomes equal to the contact angle on the channel wall. This definition is reasonable since the apparent contact angle changes during overflow (as illustrated in Figure 1c). However, the fact that the meniscus is not only pinned on the bottom edge of the channel but also on the side edges was not addressed. Therefore, indeed the apparent contact angle is also continuously changing on the side edges as well. To overcome this ambiguity, it was stated in this paper that the capillary valve was overflown when the meniscus breached the vertices formed by the channel bottom, channel side walls, and the front wall (points A and A' shown in Figure 2b). Beyond this point, the meniscus would be freely moving on the front wall and the capillary valve would no longer be useful.

Another difference between the method presented here and that in ref. [10] is the corner filling effect. In ref. [10], the meniscus was assumed to be fixed at the pinning edges. However, it was permitted to move on the front wall in this work, which allowed observation of the corner filling effect. Consequently, as the meniscus was pressurized, firstly it would tend to fill the corner formed by the top wall and the front wall instead of breaching the pinning edges and vertices A and A' (Figure 2b), which in turn would increase the apparent pressure capacity. However, this effect was not observed in the test case since the contact angles on the channel wall and the top wall were relatively large, which prevented corner filling.

The results obtained by the model presented here agrees well with the experimental results presented in ref. [10] for relatively low channel widths, which also verifies the model and the assumptions in this paper. On the other hand, the simulations carried out for comparison purposes revealed that the pressure capacity of the capillary valves can be significantly improved by decreasing the width and the height of the microchannel further.

Table 2. Comparison of the performance of the capillary valve presented in this paper with those of the similar passive valves available in the literature.

Reference	**Characteristic dimensions**	**Contact angle**	**Pressure capacity**	**Experimental /Theoretical**
Yıldırım (This paper)	width: 100 µm height: 100 µm	90º on all surfaces	~2.5 kPa	Theoretical
Chen et. al. [5]	width: 300 µm height: 60 µm	68º on all surfaces	~0.4 kPa	Theoretical
Leu and Chang [6]	width: 300 µm height: 60 µm	75º on all surfaces	~30 kPa	Experimental and theoretical
Yıldırım et. al. [9]	width: 200 µm height: 120 µm	20º on channel top, 70º on channel walls	~0.6 kPa	Experimental and theoretical
Gliere and Delattre [10]	width: 15 µm height: 15 µm	60º on channel top, 80º on channel walls	~7 kPa	Experimental and theoretical

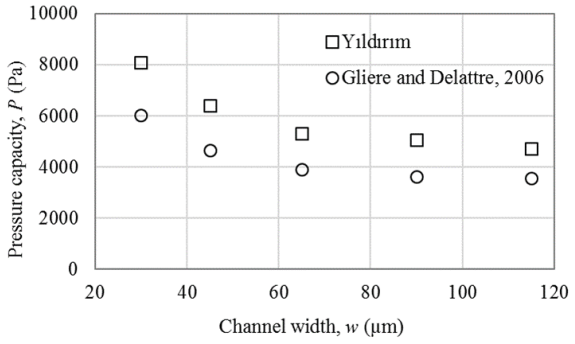

Figure 6. Pressure capacities computed by the model presented in this work (indicated by □) and the model in ref. [10] (indicated by ○). Channel height (h) is 15 µm. Contact angle on the channel wall (θ_1) is 60º and that on the top wall (θ_2) is 80º. Liquid is water with surface tension σ = 0.073 J/m^2.

As a result, it was shown that the capillary valve presented here would perform best if the contact angle on channel boundaries are 90º. It was also shown that the pressure capacity of such capillary valves could be as high as 2.5 kPa when the channel width and depth were both set to 100 µm (Figure 5). On the other hand, decreasing the channel width and depth further would significantly improve the pressure capacity (Figure 6). Comparing the values computed in this study with the ones available in the literature (Table 2) shows that the capillary valve presented here could be a promising alternative in passive microfluidic systems.

4. CONCLUSION AND DISCUSSION

In this paper, a numerical approach to determine the pressure capacity of a capillary valve was presented. Considering that the wetting properties of the microchannel material was the predominant effect in operation of the capillary valves, the method was tested for various contact angle combinations (ranging between 30º and 90º). Depending on the contact angle of the liquid on the channel material and the cover material, the shape of the menisci at the onset of the overflow and corresponding pressure capacities were determined. It was found that the valve performs best when the contact angle is 90º on all surfaces. For this contact angle value, capillary valves with different widths and depths ranging between 100 µm and 500 µm were simulated. The results showed that the pressure capacity could reach to approximately 2.5 kPa when both the channel width and the depth were 100 µm. The results were compared to those presented in the literature and the model was verified accordingly. It was shown that the pressure capacity could go up to approximately 8 kPa especially when the channel width and the channel height were significantly small (35 µm and 15 µm respectively).

The capillary valves presented here are quite useful especially in pipette operated lab-on-a-chip devices [20–22]. It is believed that the method presented here would provide a guideline for the design of such capillary valves for use in microfluidic systems.

REFERENCES

[1] Au A. K., Lai H., Utela B. R., and Folch A., "Microvalves and Micropumps for BioMEMS", ***Micromachines***, 2: 179–220, (2011).

[2] Man P., Mastrangelo C., Burns M., and Burke D., "Microfabricated plastic capillary systems with photo-definable hydrophilic and hydrophobic regions", ***International Conference on Solid-State Sensors Actuators and Microsystems***, Sendai, Japan, 1-5, (1999).

[3] Feng Y., Zhou Z., Ye X., and Xiong J., "Passive valves based on hydrophobic microfluidics", ***Sensors and Actuators A: Physical***, 108: 138–143, (2003).

[4] Cho H., Kim H.-Y., Kang J. Y., and Kim T. S., "How the capillary burst microvalve works", ***Journal of Colloid and Interface Science***, 306: 379–385, (2007).

[5] Chen J. M., Huang P.-C., and Lin M.-G., "Analysis and experiment of capillary valves for microfluidics on a rotating disk", ***Microfluidics and Nanofluidics***, 4: 427–437, (2007).

[6] Leu T.-S. and Chang P.-Y., "Pressure barrier of capillary stop valves in micro sample separators", ***Sensors and Actuators A: Physical***, 115: 508–515, (2004).

[7] Man P. P. F., Mastrangelo C. H., Burns M. A., and Burke D. T., "Microfabricated capillarity-driven stop valve and sample injector", ***Annual International Workshop on Micro Electro Mechanical Systems***, Heidelberg, Germany, 1–6, (1998).

[8] Zimmermann M., Hunziker P., and Delamarche E., "Valves for autonomous capillary systems", ***Microfluidics and Nanofluidics***, 5: 395–402, (2008).

[9] Yıldırım E., Trietsch S. J., Joore J., van den Berg A., Hankemeier T., and Vulto P., "Phaseguides as tunable passive microvalves for liquid routing in complex microfluidic networks", ***Lab on a Chip***, 14: 3334–3340, (2014).

[10] Glière A. and Delattre C., "Modeling and fabrication of capillary stop valves for planar microfluidic systems", ***Sensors and Actuators A: Physical***, 130: 601–608, (2006).

[11] Concus P. and Finn R., "On the behavior of a capillary surface in a wedge", ***Proceedings of the National Academy of Sciences***, 63: 292–299, (1969).

[12] Vulto P., Podszun S., Meyer P., Hermann C., Manz A., and Urban G. A., "Phaseguides: a paradigm shift in microfluidic priming and emptying", ***Lab on a Chip***, 11: 1596–602, (2011).

[13] Dong M. and Chatzis I., "The imbibition and flow of a wetting liquid along the corners of a square capillary tube", ***Journal of Colloid and Interface Science***, 172: 278–288, (1995).

[14] Mittelmann H. and Zhu A., "Capillary surfaces with different contact angles in a corner", ***Microgravity Science and Technology***, 1: 22-27, 1996.

[15] Brakke K. A., "The Surface Evolver", ***Experimental Mathematics***, 1: 141–165, (1992).

[16] Lei K.F., "Materials and Fabrication Techniques for Nano- and Microfluidic Devices", Microfluidics in Detection Science : Lab-on-a-chip Technologies, ***The Royal Society of Chemistry***, Cambridge, UK, (2014).

[17] Duffy D. C., McDonald J. C., Schueller O. J., and Whitesides G. M., "Rapid Prototyping of Microfluidic Systems in Poly(dimethylsiloxane)", ***Analytical Chemistry***, 70: 4974–4984, (1998).

[18] Becker H., "Polymer microfluidic devices", ***Talanta***, 56: 267–287, (2002).

[19] Myshkis A. D., Babskii V. G., Kopachevskii N. D., Slobozhanin L. A., and Tyuptsov A. D., "Low-Gravity Fluid Mechanics, Mathematical Theory of Capillary Phenomena", ***Springer-Verlag***, 1, Berlin, (1987).

[20] Kasap E. N., Çoğun F., Yıldırım E., Boyacı İ. H., Çetin D., Suludere Z., Tamer U., and Ertaş N., "Microchip Based Determination of Bacteria by In-chip Sandwich Immunoassay", ***International Multidisciplinary Symposium on Drug Research and Development***, Eskişehir, Turkey, 89, (2015).

[21] Doğan Ü., Kasap E., Çoğun F., Yıldırım E., Çetin D., Suludere Z., Boyacı İ. H., Ertaş N., and Tamer U., "Simultaneous Detection of Two Different Bacteria Using QDs and MNPs", ***International Conference: 10th Aegean Analytical Chemistry Days***, Çanakkale, Turkey, 365, (2016).

[22] Ahi E. E., Gümüştaş A., Çiftçi H., Çağlayan M. G., Selbes Y. S., Çoğun F., Yıldırım E., and Tamer U., "Chip-Based Immunomagnetic Separation of Human Chorionic Gonadotropin", ***International Conference: 10th Aegean Analytical Chemistry Days***, Çanakkale, Turkey, 361, 2016.